

A DESIGN METHOD FOR ROBUST AUTOMOTIVE AND AEROSPACE COMPOSITE STRUCTURES INCLUDING MANUFACTURING VARIATIONS

AUTHOR: Dr Dirk Lukaszewicz, BMW AG, Research and Innovation Centre, Knorrstraße 147, 80788 München, Germany, Email: Dirk.Lukaszewicz@bmw.de

Paper Number: 15-0135

ABSTRACT

Objective

Composites may enable further weight reductions for plastic composite intensive vehicles. Among the challenges associated with greater adoption of composites in the automotive industry are the need for novel design procedures, the use of composites in impact applications and the greater variability during composite manufacture. Here, a method is presented to account for composite manufacturing variability in the design phase.

Methods

The method is based on measuring the variability in a part and the translation into a simulation. As an example a side-pole impact into a doorsill subassembly was chosen. The test data are used to validate numerical simulation models for the impact situation. The simulation is then used to study the sensitivity of the system with respect to manufacturing variability. A novel optimization was also used that decouples multiple manufacturing variations and allows identifying limits on acceptable variability levels.

Results

The experimental tests exhibit changes in mechanical performance due to the existence of manufacturing variations. The numerical simulation including these manufacturing variations shows reasonable agreement with the experimental data. The FE model was then used to vary the manufacturing variations and to identify allowable intervals within defined performance criteria.

Conclusion

The design methodology has significant benefits for automotive composite design and manufacturing since it may enhance the robustness of composite crash-structures, reduce part cost and eliminate excessive safety factors to account for unknown manufacturing variations.

KEY WORDS: Crash, Crashworthiness, Finite Elements, Vehicle Design

INTRODUCTION

To enable further weight reductions and fuel savings for future vehicles, Plastic Composite Intensive Vehicles (PCIVs) (Barnes, Coles, Roberts, Adams, & Garner 2011) may become more widespread. Advanced Fibre Reinforced Plastics (FRPs) exhibit excellent mechanical and crash performance when compared with conventional metallic structures. Both the specific stiffness and energy absorption capability of FRPs exceed common automotive materials, such as aluminium and steel, making them highly suitable for crash application for frontal, side and rear impact.

However, composites exhibit different deformation behaviour than steel or aluminium, thus requiring an adaptation of design philosophies for vehicle safety (Ferenczi, Kerscher, & Möller 2014). In addition, FRP mechanical performance may vary significantly due to manufacturing variations (MV) such as fibre misalignment, fibre waviness, gaps or folding. Safe structural design of composite vehicles containing MVs may thus require enhanced design methods and processes. An example for this is introduced here.

Impact Of Imperfections On Mechanical Performance

Some of the most common MVs are fibre misalignment, fibre waviness, laps and gaps, and porosity. The focus of this work will be on preforming MVs, which include in- and out-of-plane waviness and longitudinal and transverse folding. An early study into the impact of fibre waviness by Mrse and Piggott (Mrse & Piggott 1993) studied the compressive properties of thermoplastic carbon fibre prepreg, which had some initial waviness and were crimped to introduce additional waviness. The authors observed some reduction in compression modulus but a significant reduction of compressive strength with increasing wave character.

Daniel and co-workers (Chun, Shin, & Daniel 2001; Hsiao & Daniel 1996a, 1996b) focused on the impact of fibre waviness on the elastic properties of carbon-fibre reinforced epoxy prepreg. An analytical model was used to evaluate the impact of waviness on tensile and shear modulus as well as Poisson's ratio. In-plane tensile modulus was found to degrade significantly as a function of waviness, up to 35% for a graded wave with characteristic value of 0.1, while transverse in-plane tensile modulus were found to increase.

Compressive stiffness and strength were more significantly affected and the reduction in compressive strength could be up to 80% for a graded wave with a characteristic value of 0.1. Similar observations were made for Poisson's ratios and shear moduli. Trends were consistent for uniform and graded waviness but significantly less pronounced for localized waviness, which had only a small impact on overall property changes. Garnich and Karamani (Garnich 2005; Garnich & Karamani 2004a, 2004b) used Finite Element (FE) simulations to demonstrate that fibre waviness had increasing impact on mechanical performance with increasing fibre misalignment and obtained stiffness reductions of up to 70%. Chan and Chou (Chan & Chou 1995) studied the impact of misalignment on the flexural properties of laminates and observed that waviness yielded more severe stiffness and strength reductions in highly stressed plies.

Most of this early numerical work assumed either some form of symmetry, such as a sinusoidal waviness, or that the waviness would be confined. However, as mentioned previously out-of-plane waviness may affect neighbouring plies making it very difficult to separate the effects of waviness in individual plies. For example, Joffe et. al. (Joffe, Mattsson, Modniks, & Varna 2005) studied the mechanical properties and deformation behaviour of NCF using both FE-models and extensive testing proposing a linear approximation between misalignment angle and obtaining a reduction of 40% in mechanical performance for a misalignment angle of 15°. A linear relationship between MV and mechanical property had previously not been predicted. In addition the reduction was lower than what might have been expected. Pansart, Sinapius and Gabbert (Pansart, Sinapius, & Gabbert 2009) presented a coupled FEM/analytical approach to study the impact of both fibre misalignment and fibre waviness on the compressive strength of NCF and reported increasing reductions in compressive strength with increasing fibre waviness angle and wave half wavelength of up to 40% for 10deg waviness and a half wavelength of 5. El-Hajjar and Petersen (El-Hajjar & Petersen 2011) proposed a new approach to model waviness using a Gaussian function as opposed to the sinusoidal approach used previously and tested the tensile stiffness and strength of wavy laminates with reported strength reductions of up to 60%. Potter and co-workers (Bloom, Wang, & Potter 2013; Lightfoot, Wisnom, & Potter 2013a, 2013b) have studied waviness including wrinkles experimentally and observed a reduction of up to 50% for the tensile strength. While most of the experimental work thus tends to confirm the initial analytical predictions we can conclude that experimentally measured reductions in mechanical properties are lower than the predictions from early models. In addition most experimental results tend to show a linear relationship between MV characteristics and mechanical property.

Since the focus of this work is the crashworthiness of composite vehicle structure an important aspect is the impact of such MVs during dynamic deformation as opposed to the quasi-static tests commonly employed. This has been studied by Hsiao and Daniel (Hsiao & Daniel 1999) for fibre waviness. It was demonstrated that the effect of waviness was less severe for increasingly dynamic loading due to the strain rate dependent increase in

stiffness. It can thus be concluded that the used of quasi-static test data to model the impact of MVs on the crashworthiness will represent a conservative estimate.

METHODS

Two sets of carbon fibre reinforced plastic (CFRP) subassemblies of a doorsill were manufactured with different MV distributions. The sets were then mechanically tested to measure the maximum deformation into the doorsill assembly, representing a loading situation comparable to an FMVSS214 side pole impact (Anon 1998). Additionally, MVs were recorded through destructive testing and the information was incorporated into a numerical simulation to replicate the test results. The simulation was then validated against the test data. Based on this validated FE simulation a method is introduced that enables direct simulation of MVs and their impact on structural performance for a side pole impact. Latin hypercube (LHC) sampling is then used to vary the characteristics of the MV. The sampling results are then used to generate an analytical regression model. A novel optimization method is then used that aims at finding the largest hyperbox containing good designs within the solution space, thus generating limits on the characteristics of the MV.

Component Manufacture

The subassembly studied here is the side frame of a composite vehicle body structure made from carbon fibre reinforced epoxy. Within the vehicle architecture one of the functions of the side frame is protection of the passengers in an impact event, such as a side pole test. During a side pole test the intrusion into the passenger cell have to be mitigated, while the supplementary restrained systems, i.e. airbags and curtains, are being deployed and the vehicle is stopped at the pole.

This occurs while the side frame undergoes significant deformation, which can exceed 100mm locally. To prevent large deformations of the side frame the incoming loads are normally redistributed in the floor structure and then to the vehicle non-struck side. Consequently, the side frame is supported by cross members and ancillary structural elements, which enable load transfer to the non-struck side of the impact, Figure 1. The side frame is an assembly of individual parts through co-curing for the inside and outside parts and adhesive bonding for the inside and outside. The key components under investigation here are the inner and outer doorsill parts, the inner reinforcement and the inner top cap and frontal cap, five parts in total, Figure A 1. This assembly is referred to as side frame-set of which a total of six was manufactured for two different MV combinations, referred to as “A” and “B”. To manufacture parts with different MV severities and types the temperature of the mould as well as the mounting of the plies in the frame was modified. Of the six side frame-sets each, three were visually inspected and three were cured with resin and tested mechanically. This way it was ensured that the side frame-sets for inspection and mechanical inspection were from the same batch. This was important as the MVs were assumed to be identical between visually inspected and mechanically tested subassemblies. For visual inspection the parts were segmented into plies again and for each segment the MV’s in the plies were recorded. To record the MV’s a grid with a side length of 50x50mm was projected onto the vehicle in all projection planes. Here we are concerned with a side frame subassembly only and consequently only the y-z-vehicle plane is used to record MV’s. For each ply the part was then inspected visually progressing from one quadrant of the grid to the next.

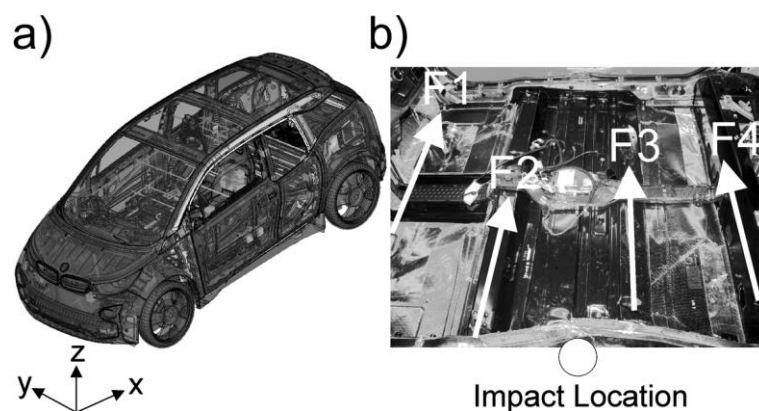


Figure 1a) Overview of the vehicle layout and coordinate system with the side frame highlighted and b) Illustration of principal loading of a doorsill in a side pole impact. The loading conditions are comparable to a five point bending configuration.

For each quadrant the in- and out-of-plane waviness, longitudinal and transverse folding amongst other MV's such as tearing of the stitching yarn was recorded. Then each MV was categorized according to its characteristics, with six different characteristics categories for each MV. The categories are dependent on the MV type but can generally be related to physical variables for a given MV, for example for waviness the MV category is related to the waviness height and length. This process for both MV locations as well as MV characteristics was then carried out by three different quality inspection staff to ensure that all MVs were recorded and that the characteristics was recorded correctly. In case of disagreement between individual recordings the defect with the highest severity was retained. This process was then repeated for each ply in the part and for all three produced parts. The result was a feature map for all three parts combined for every ply were both the location of the MV's as well as their characteristics could be easily accessed. Table 1 provides an overview of the recorded MVs that were used in this study to develop the simulation model.

Table 1: Varied MVs and Characteristic Range. The Characteristic Range is a normalized classification relating to the physical dimensions or shape of a given MV.

MV	Out-of-plane waviness	In-plane waviness	Longitudinal Folding	Transverse Folding
Size Range	1-6	1-6	1-6	1-6

Testing

The principal loading of a side frame in a vehicle may be approximated using a five-point bending configuration, Figure 1. Consequently, the test set-up was designed to replicate this vehicle situation as shown in Figure 2. A loading frame consisting of two supports on the lower and two supports on the upper side was manufactured. The mounting positions were equipped with machined interfaces that would fit the complex geometry of the doorsill and would prevent torsion and bending while allowing some transverse movement. The entire setup with the side frame section mounted into the loading frame was placed into a drop tower where an impactor with a diameter of 254mm would impact the side frame in the same position as the side pole in a full vehicle test. An accelerometer on the impactor was used after testing to calculate the force on the impact side. A laser beam system was used to measure the displacement of the impactor. This was levelled to zero on top of the side frame for each test. The loading frame was then aligned with the impactor and fixed to the ground to prevent further movement during testing.

An initial FE simulation was setup to generate a test configuration, were the load level and energy absorption of the side frame were comparable to the full vehicle loading. From the FE-simulation a total drop weight of 352kg and a test speed of 5.65m/s were found to be comparable to the full vehicle-loading situation. For each feature map "A" and "B" three side frames were tested and the acceleration and displacement at the impactor were recorded. After recording, the data were filtered using a Butterworth filter with a channel frequency class of 60 (Anon 1995). The experimental results are summarized in Table 2.

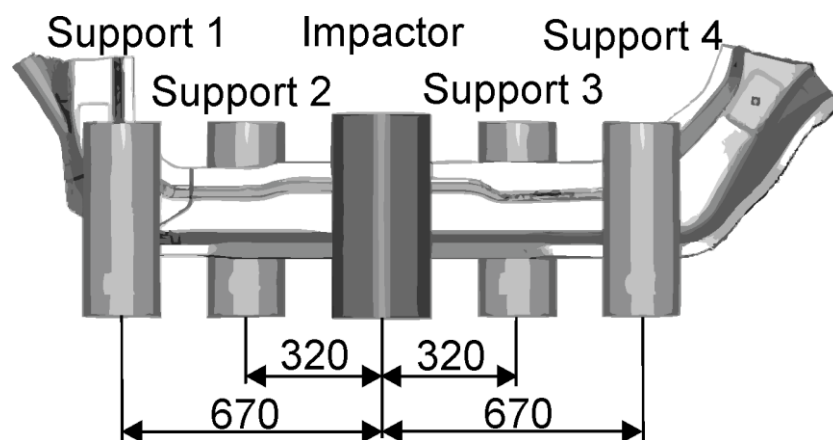


Figure 2: Test setup for dynamic five-point-bending of a doorsill in a drop tower.

Table 2: Experimental Results. The labels “A” and “B” designate two subassembly configurations with known, but different MVs in the parts.

Test [-]	Maximum Intrusion [mm]	Mean [mm]	
A1	99.7		
A2	101.9	101.1	± 1.2
A3	101.7		
B1	111.4		
B2	105.7	108.9	± 3.0
B3	109.7		

FE Model with Manufacturing Variations

To replicate the experimental results a baseline model was set up in the commercial FE-Code Abaqus 6.11-2A (*Dassault Simulia 2013*). The composite parts were modelled using the ABQPly-Fabric composite material model within Abaqus using a single shell element over the thickness incorporating the physical layers into a shell section. Typical mesh size was 10mm for the composite parts. In total the model consists of 240613 elements, while the composite parts were modelled using 67107 shell elements of the type S4R. The composite parts stacking sequence, ply thickness and ply orientation were modelled as composite sections with an offset from the respective shell element plane. The inner and outer side frame were glued together, this was modelled by cohesive elements along the bond line, which had energy based material degradation behaviour.

The Impactor and the four supports were modelled as rigid bodies. The impactor had a reference node on the perimeter in line with the impact point to enable simple comparison with experimental results. All six degrees of freedom of the supports were fixed. The impactor was attached to a reference point, with an impact mass of 352kg and the impact velocity of 5.65m/s as initial condition with displacement in the z-direction (vehicle y-direction) only. Total simulation time was 0.7s. Forces and displacements from the simulation were measured at the reference node, which was identical to the accelerometer location in the physical test. To translate the MVs from visual inspection onto the FE-model material definitions were necessary. These were generated through extensive mechanical testing of coupons, for example in tension and compression. The generation of these FE material definitions are not the focus of this paper. As a result specific material data for different MV types and their characteristics were available.

The MV’s from specimen manufacture that were translated into the FE model were in- and out-of-plane waviness, longitudinal and transverse folding, Table 1. The mapping of the MV’s was scripted in ANSA (*Beta CAE 2014*). First the visual inspection data was used to segment the side frame into areas with different material behaviour, depending on whether defects were present or not and taking into account individual plies as well. This information was recorded in the shell section definition of each element by modifying the material definition of all the affected plies. As an example in one element the third ply and sixth ply might be associated with in-plane waviness material definition while all remaining plies would retain their nominal material definition. A neighbouring element might be associated with through-thickness waviness in the 4th to 6th ply of the shell section.

Then, for each area the plies were associated with the corresponding MV severity ranging from 1 to 6 from the visual inspection data. The result is a model with a significant number of unique shell sections.

This is illustrated in Figure A 2 where the different shell section definitions are shown through colour coding. The grey area contains nominal material properties, while the coloured areas are associated with MVs in the shell sections. Since data from multiple preforms and inspectors were mapped simultaneously an approach was needed to identify which MVs would be mapped onto the final simulation part. As mentioned previously the aim was to map the most severe MV onto the geometry. Here a stiffness based mapping approach was used, where the MV’s were ranked according to their combined impact on tensile and compressive stiffness in the fibre direction, E_{11+} and E_{11-} . The plies were then associated with appropriate material definitions, which were generated through testing. Since material definitions for out-of-plane waviness were not available the material definition for in plane waviness was used here as well.

Optimization

The goal of the optimisation proposed here is to simultaneously define allowables for multiple optimisation goals, such as multiple MVs. In other words the process is aimed at defining a maximum solution space. To achieve this, the approach proposed by Zimmermann and Edler von Hoessle (Zimmermann & von Hoessle 2013) is adapted here for the optimisation of composite structural MVs. The optimization algorithm by

Zimmermann and Edler von Hoessle combines stochastic sampling and Bayesian interference to generate a feasible maximum solution space.

Initially, a good design is created using classical optimization techniques such as gradient based optimization or genetic algorithms (GA). Starting from this good design a randomly defined search box is populated with sampling points. The iteration can be divided into two phases, Phase 1 and Phase 2.

In the first phase the search box is generated and the results are evaluated with respect to a performance criterion, for example the maximum intrusion. By removing poor designs from the initial search box the largest possible box is computed that contains no poor designs and a maximum of good designs. This may not necessarily be the largest bounding box for all good designs. In additional steps this box is extended or reshaped and new Latin Hypercube samples in the bounding box are calculated. This process is repeated until the bounding box is stationary and at maximum size.

In the second phase new samples are generated inside the box and the box is shrunk or reshaped until the bounding box contains only good designs. The new box is then populated again using Latin Hypercube sampling. This process is repeated until a number of consecutive Latin Hypercube seeds within a bounding box produce only good designs, after which the process is stopped.

Performance criterion: Since the optimization approach described above uncouples all MVs, which are simulated simultaneously, it is possible to generate allowable intervals for each MV independent of the others. All repeated tests including full vehicle crash tests exhibit a standard deviation that is their tests results vary to a certain extent between nominally identical tests. This may be due to the fact that no vehicle undergoing testing is free of MVs, variability in the test facility or the accuracy of the measurement equipment to name a few here, this fact is being used as definition for the performance criterion for the MV optimization. If the scatter between two nominally identical tests is equal to or greater than the change in performance that can be attributed to different MVs in the vehicle, then MVs are having an insignificant impact on vehicle performance since a distinction between scatter due to MVs and the test configuration cannot be made. This may be defined as

$$\Delta d_{MV} \leq \Delta d_{Test} \quad (1)$$

where Δd_{MV} is the relative change in Intrusion due to MV's and Δd_{Test} is the relative change between tests. While this repeatability of the BMW test facility is established it is not being used in this paper for confidentiality reasons. Instead, the scatter of the impact tests for side frame configuration "A" of 1.2% is being used here. This value has no connection to the repeatability of the full vehicle test facility and is simply used here to illustrate the process. Since the base simulation without any MVs had a maximum intrusion of 97.6mm, the maximum allowable intrusion in a model containing any MVs is 98.8mm.

Workflow: The following section introduces a workflow, which controls the creation, execution and result handling for the FE simulation and optimization. The goal of the optimization procedure is to identify allowable intervals for MVs, which will ensure that the variability of the response, or intrusion, stays within certain limits.

The optimization workflow is shown in Figure A 3. The optimization starts with the setup of the initial model. Here all MVs are mapped onto the respective locations on the part and plies as described previously for the validation simulation. Lastly, all characteristics are set to zero, i.e. the material card without knockdown is used to calculate the baseline result for the simulation. From this model variants are then generated using a scripted Latin Hypercube simulation approach. By varying the characteristics of the MVs 400 variants were generated. They location on the part and the ply was fixed. The models were then solved in parallel on an HPC Cluster with 16 CPUS for variant. Abaqus Explicit 6.11-2A was used as solver. Typical runtime was 75 minutes.

From the simulation the intrusion of the Impactor was evaluated as Latin Hypercube Output. The nodal displacement of the impactor was extracted using a python script and the maximum value was recorded. ClearVuAnalytics (Divis 2014) was then used to generate a Response Surface Model (RSM). From the available methods within the software the random forest tree algorithm consistently generated the highest degree of correlation R^2 between the FE-data and the regression model for the optimization. It was thus used to compute the RSM. Allowable intervals for the MV characteristics were then calculated based on the RSM using the bounding box optimization described previously. This process was then repeated by setting the maximum severity of the MV characteristics to the allowable intervals from the previous optimization. Here, the process was stopped after two iterations. Lastly, the allowable intervals from the optimization were validated using 10 FE simulations with discreet MV characteristics.

RESULTS

The FE-simulation was computed using Abaqus 6.11-2A on 16 cores with double precision. Results are shown in Figure 3.

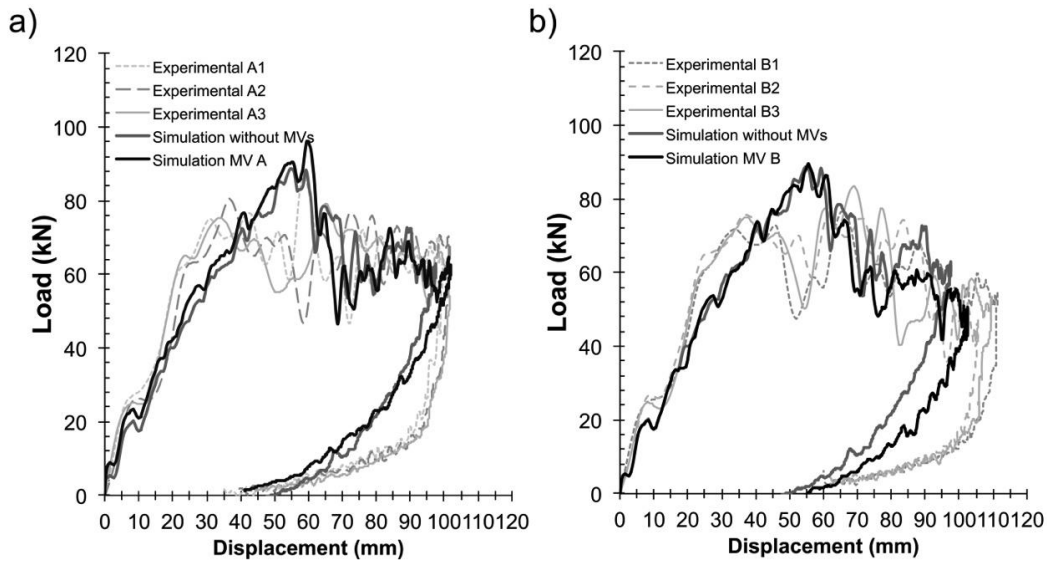


Figure 3a): Experimental and numerical load-displacement curves for MV's for subassembly A with comparison to the baseline simulation and MV simulation and b) for subassembly B.

The base simulation without any MV's yielded a maximum intrusion of 97.6mm, 101.9mm for MV map A and 102.5mm for MV map B. When comparing the simulation results with the experimental results in Table 2 it can be seen that the simulation replicates the experimental results well for MV map A, while it significantly under predicts the experimental results for MV map B. This may be explained through the fact that now all MVs are mapped and that the mapping of through-thickness waviness is based on the material data for in-plane waviness. For the subsequent optimization of the limiting samples for each part model A was used.

Two consecutive iterations of the Latin Hypercube Simulation Process were conducted to develop the analytical model for the MV optimization. From the first 400 variants that were generated for the Latin Hypercube simulation 391 design points were simulated successfully. Based on this data set an analytical model was generated using a random forest algorithm. The R^2 of the RSM was 0.91. For the second 400 variants the R^2 of the RSM was 0.9. The results of the Latin Hypercube simulation are summarized in Table A 1. The results of the corridor calculation are shown in Table 3. The numbers indicate the allowable intervals for the MVs characteristic for each MV.

DISCUSSION

The optimization generates limits on the maximum characteristics of the MV that do not detrimentally affect mechanical performance. The optimization demonstrates that MVs have different bearing on the change in functional performance, which is governed by both the characteristics of the MV, such as the angle of fibre waviness, as well as the location. The method thus enables safe structural design of advanced composites by linking manufacturing and structural design.

Variability of the MV location was typically very low since the MV locations remained relatively constant for all visually inspected side frames. MV characteristics fluctuated, which could be explained amongst other things by the variability of the areal weight of the incoming NCF. This validates the assumption that the MV location in the mechanically tested side frames is comparable to the visually inspected side frames.

Table 3: Allowable Intervals for the MV Characteristics investigated in the FE simulation and optimization.

MV	Out-of-plane waviness	In-plane waviness	Longitudinal Folding	Transverse Folding
First Iteration	3	5	6	6
Second Iteration	3	5	6	6
Final	2	3	5	4

This is a significant shortcoming of the results presented herein, and further work is aimed at addressing this in the future (Deobald et al. 2014). Further, it should be noted that not all manufacturing variations present in the as manufactured side frames were translated into the model.

One interesting result is the fact that certain combinations of manufacturing variations result in a reduction of the maximum intrusion. There are several possible explanations for this that need to be explored further. The first would be numerical noise, for example due to different domain decompositions for various models. The second is the fact that certain MV's, such as longitudinal and transverse folding as well as in-plane waviness can actually improve the stiffness of a ply either in the fibre direction or transverse which may improve stiffness locally and this effect was also captured by the FE model. The third explanation would be a change of failure sequence due to MV's which would result in a redistribution of the load on a part and could change the severity of a MV, this effect is explored in more detail for out-of-plane waviness in another paper (Deobald et al. 2014).

Here, a novel concept for designing composite structures has been shown which is based around optimization of the entire product development including manufacturing. Historically, most MVs in composite parts are not accepted because they may be detrimental to safety and are difficult to reproduce in a serial prototype-manufacturing environment often encountered in the aerospace industry. In addition, they are detrimental to achieving ultimate lightweight designs. However, ultimate lightweight design is not desirable if cost and production volume constraints are taken into account. Consequently, designing with MVs becomes a potential target for improving the composite development process with respect to automotive requirements. Potential improvements include a direct link between manufacturing and design to simultaneously optimize both. Further, design with MVs may enable a trade-off between lightweight design, cost and production volume. A workflow that enables safe structural design with MVs is demonstrated here for a generic composite crash structure. An approach for translating MVs from testing into an FE simulation is first shown. The FE model that was developed here demonstrated reasonable correlation between the simulated and experimentally observed structural response for two representative MVs maps. One model was then subsequently used to optimize the manufacturing variations with respect to their impact on structural performance. The method and simulation approach shown herein may enable significant improvements to production cost, rate and part quality for composites components for the aerospace and automotive industry.

ACKNOWLEDGEMENTS

The author would like to thank BMW Group for the opportunity to carry out and publish this research. The author acknowledges the support from David Becherer, Viorel-Constantin Ionescu and Dr Stefan Kerscher from the BMW Group. The author would also like to thank Lyle Deobald, Chul Y. Park, Nihar Desai and Mary Matthews from the Boeing Company for the invaluable feedback and discussions.

REFERENCES

- Anon. (1995). Instrumentation for impact test - Part 1 - Electronic Instrumentation (Vol. J211-1): SAE International.
- Anon. (1998). U.S. Department of Transportation: Federal Motor Vehicle Safety Standards and Regulations. Retrieved 23rd February 2013, from <http://www.nhtsa.gov/cars/rules/import/fmvss/index.html>
- Barnes, G., Coles, I., Roberts, R., Adams, D. O., & Garner, D. M. J. (2011). Crash Safety Assurance Strategies for Future Plastic and Composite Intensive Vehicles (PCIVs). Cambridge, Massachusetts, USA: Volpe National Transportation Systems Centre.
- Beta CAE. (2014). ANSA.
- Bloom, L., Wang, J., & Potter, K. (2013). Damage progression and defect sensitivity: An experimental study of representative wrinkles in tension. *Composites Part B*, 45(1), 449-458.
- Chan, W., & Chou, C. (1995). Effects of delamination and ply fibre waviness on effective axial and bending stiffness's in composite laminates. *Composite structures*, 30, 299-306.
- Chun, H. J., Shin, J. Y., & Daniel, I. M. (2001). Effects of material and geometric nonlinearities on the tensile and compressive behaviour of composite materials with fibre waviness. *Composites Science And Technology*, 61(1), 125-134.
- Dassault Simulia. (2013). Abaqus 6.11-2A.
- Deobald, L., Park, C., Desai, N., Ramnath, M., Jin, O., Lukaszewicz, D., & Kerscher, S. (2014). *Simulation of Composite Manufacturing Variations to Determine Stiffness and Strength Reductions in Automotive and Aerospace Structure*. Paper presented at the ACS 29th Technical Conferences, San Diego
- Divis. (2014). ClearVu Analytics.
- El-Hajjar, R. F., & Petersen, D. R. (2011). Gaussian function characterization of unnotched tension behaviour in a carbon/epoxy composite containing localized fibre waviness. *Composite structures*, 93(9), 2400-2408.

- Ferenczi, I., Kersch, S., & Möller, F. (2014). *Energy Dissipation and structural integrity in frontal impact*. Paper presented at the 23rd ESV 2013 International Technical Conference on the Enhanced Safety of the Vehicles, Seoul, Korea.
- Garnich, M. (2005). Localized Fibre Waviness and Implications for Failure in Unidirectional Composites. *Journal Of Composite Materials*, 39(14), 1225-1245.
- Garnich, M., & Karami, G. (2004a). Finite element micromechanics for stiffness and strength of wavy fibre composites. *Journal Of Composite Materials*, 38, 273.
- Garnich, M., & Karami, G. (2004b). Finite Element Micromechanics for Stiffness and Strength of Wavy Fibre Composites. *Journal Of Composite Materials*, 38(4), 273-292.
- Hsiao, H. M., & Daniel, I. M. (1996a). Effect of fibre waviness on stiffness and strength reduction of unidirectional composites under compressive loading. *Composites Science And Technology*, 56, 581-593.
- Hsiao, H. M., & Daniel, I. M. (1996b). Elastic properties of composites with fibre waviness. *Composites Part A-Applied Science And Manufacturing*, 27, 931-941.
- Hsiao, H. M., & Daniel, I. M. (1999). *Effects of strain rate and fibre waviness on the compressive behaviour of composite laminates*. Paper presented at the ICCM-12, Paris France.
- Joffe, R., Mattsson, D., Modniks, J., & Varna, J. (2005). Compressive failure analysis of non-crimp fabric composites with large out-of-plane misalignment of fibre bundles. *Composites Part A: applied science and manufacturing*, 36, 1030-1046.
- Lightfoot, J. S., Wisnom, M. R., & Potter, K. (2013a). Defects in woven preforms: formation mechanisms and the effects of laminate design and layup protocol. *Composites Part A*, 1-35.
- Lightfoot, J. S., Wisnom, M. R., & Potter, K. (2013b). A new mechanism for the formation of ply wrinkles due to shear between plies. *Composites Part A*, 49(C), 139-147.
- Mrse, A., & Piggott, M. (1993). Compressive properties of unidirectional carbon fibre laminates: II. The effects of unintentional and intentional fibre misalignments. *Composites Science And Technology*, 46, 219-227.
- Pansart, S., Sinapius, M., & Gabbert, U. (2009). A comprehensive explanation of compression strength differences between various CFRP materials: Micro-meso model, predictions, parameter studies. *Composites Part A*, 40(4), 376-387.
- Zimmermann, M., & von Hoessle, J. (2013). Computing solution spaces for robust design. *International Journal for Numerical Methods in Engineering*, 94(3), 290-307.

APPENDIX

Table A 1: Latin Hypercube Simulation Results And No. Of Designs above Critical Limit

Iteration	R ²	Misclassifications [-]	Misclassifications [%]
1st	0.91	125	31.9
2nd	0.90	72	18.3
Final	-	43	10.8

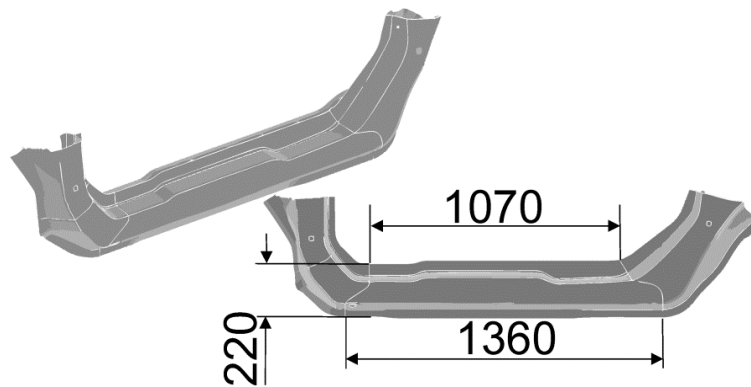


Figure A 1: Segment of a side frame and overall dimensions of the doorsill section.

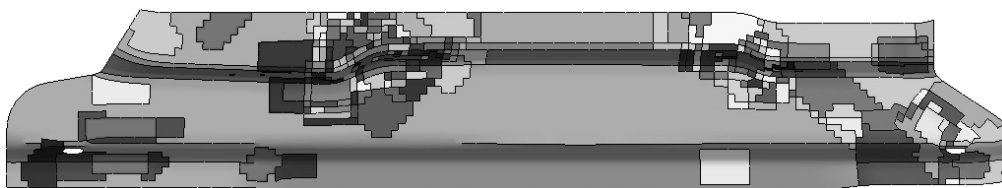


Figure A 2: Example of a simulation model for the doorsill outside with mapped MV's. The patches on the parts represent discrete material definitions for the respective elements.

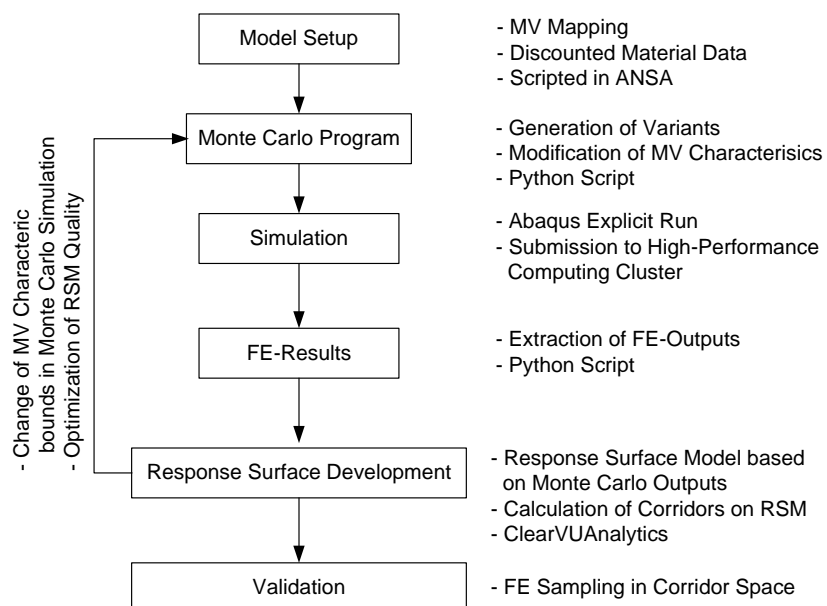


Figure A 3: Simulation Workflow for the MV corridors and the maximum allowable characteristic. The right-hand side description provides details of the operations for each step of the simulation workflow.